

FEATURES

- Fully differential**
- Low noise**
 - 2.25 nV/ $\sqrt{\text{Hz}}$
 - 2.1 pA/ $\sqrt{\text{Hz}}$
- Low harmonic distortion**
 - 98 dBc SFDR at 1 MHz
 - 85 dBc SFDR at 5 MHz
 - 72 dBc SFDR at 20 MHz
- High speed**
 - 410 MHz, 3 dB BW (G = 1)
 - 800 V/ μs slew rate
 - 45 ns settling time to 0.01%
- 69 dB output balance at 1 MHz**
- 80 dB dc CMRR**
- Low offset: ± 0.5 mV maximum**
- Low input offset current: 0.5 μA maximum**
- Differential input and output**
- Differential-to-differential or single-ended-to-differential operation**
- Rail-to-rail output**
- Adjustable output common-mode voltage**
- Wide supply voltage range: 5 V to 12 V**
- Available in a small SOIC package and an 8-lead LFCSP**

APPLICATIONS

- ADC drivers to 18 bits**
- Single-ended-to-differential converters**
- Differential filters**
- Level shifters**
- Differential PCB drivers**
- Differential cable drivers**

GENERAL DESCRIPTION

The AD8139 is an ultralow noise, high performance differential amplifier with rail-to-rail output. With its low noise, high SFDR, and wide bandwidth, it is an ideal choice for driving analog-to-digital converters (ADCs) with resolutions to 18 bits. The AD8139 is easy to apply, and its internal common-mode feedback architecture allows its output common-mode voltage to be controlled by the voltage applied to one pin. The internal feedback loop also provides outstanding output balance as well as suppression of even-order harmonic distortion products. Fully differential and single-ended-to-differential gain configurations are easily realized by the AD8139. Simple external feedback networks consisting of four resistors determine the closed-loop gain of the amplifier.

Rev. C

[Document Feedback](#)

Information furnished by Analog Devices is believed to be accurate and reliable. However, no responsibility is assumed by Analog Devices for its use, nor for any infringements of patents or other rights of third parties that may result from its use. Specifications subject to change without notice. No license is granted by implication or otherwise under any patent or patent rights of Analog Devices. Trademarks and registered trademarks are the property of their respective owners.

FUNCTIONAL BLOCK DIAGRAMS

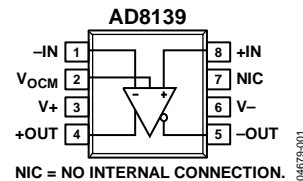


Figure 1. 8-Lead SOIC

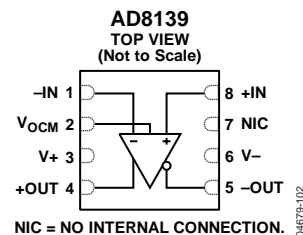


Figure 2. 8-Lead LFCSP

The AD8139 is manufactured on the proprietary Analog Devices, Inc., second-generation XFCB process, enabling it to achieve low levels of distortion with input voltage noise of only 2.25 nV/ $\sqrt{\text{Hz}}$.

The AD8139 is available in an 8-lead SOIC package with an exposed paddle (EP) on the underside of its body and a 3 mm \times 3 mm LFCSP. It is rated to operate over the temperature range of -40°C to $+125^{\circ}\text{C}$.

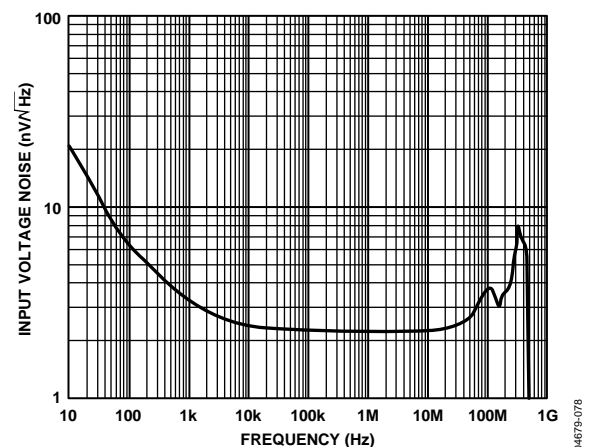


Figure 3. Input Voltage Noise vs. Frequency

TABLE OF CONTENTS

Features	1	Pin Configurations and Function Descriptions	8
Applications	1	Typical Performance Characteristics	9
General Description	1	Test Circuits	18
Functional Block Diagrams	1	Theory of Operation	19
Revision History	2	Typical Connection and Definition of Terms	19
Specifications	3	Applications Information	20
$V_S = \pm 5\text{ V}$, $V_{OCM} = 0\text{ V}$	3	Estimating Noise, Gain, and Bandwidth with Matched	
$V_S = 5\text{ V}$, $V_{OCM} = 2.5\text{ V}$	5	Feedback Networks	20
Absolute Maximum Ratings	7	Outline Dimensions	25
Thermal Resistance	7	Ordering Guide	26
ESD Caution	7		

REVISION HISTORY

6/2016—Rev. B to Rev. C

Changed CP-8-2 to CP-8-13	Throughout
Changes to Figure 1 and Figure 2	1
Changes to Figure 5, Figure 6, and Table 5	8
Updated Outline Dimensions	25
Changes to Ordering Guide	26

10/2007—Rev. A to Rev. B

Changes to General Description Section	1
Added Figure 2; Renumbered Sequentially	1
Changes to Table 1	3
Changes to Table 2	5
Changes to Table 6 and Layout	8
Added Figure 6	8
Changes to Figure 30	12
Changes to Layout	17
Changes to Figure 63	22
Changes to Exposed Paddle (EP) Section	23
Updated Outline Dimensions	24

8/2004—Rev. 0 to Rev. A

Added 8-Lead LFCSP	Universal
Changes to General Description Section	1
Changes to Figure 2	1
Changes to $V_S = \pm 5\text{ V}$, $V_{OCM} = 0\text{ V}$ Specifications	3
Changes to $V_S = 5\text{ V}$, $V_{OCM} = 2.5\text{ V}$ Specifications	5
Changes to Table 4	7
Changes to Maximum Power Dissipation Section	7
Changes to Figure 26 and Figure 29	12
Added Figure 39 and Figure 42; Renumbered Sequentially	14
Changes to Figure 45 to Figure 47	15
Added Figure 48	15
Changes to Figure 52 and Figure 53	16
Changes to Figure 55 and Figure 56	17
Changes to Table 6	19
Changes to Voltage Gain Section	19
Changes to Driving a Capacitive Load Section	22
Changes to Ordering Guide	24
Updated Outline Dimensions	24

5/2004—Revision 0: Initial Version

SPECIFICATIONS

 $V_S = \pm 5\text{ V}$, $V_{OCM} = 0\text{ V}$ $T_A = 25^\circ\text{C}$, differential gain = 1, $R_{L, dm} = 1\text{ k}\Omega$, $R_F = R_G = 200\ \Omega$, unless otherwise noted. T_{MIN} to $T_{MAX} = -40^\circ\text{C}$ to $+125^\circ\text{C}$.

Table 1.

Parameter	Test Conditions/Comments	Min	Typ	Max	Unit
DIFFERENTIAL INPUT PERFORMANCE					
Dynamic Performance					
–3 dB Small Signal Bandwidth	$V_{O, dm} = 0.1\text{ V p-p}$	340	410		MHz
–3 dB Large Signal Bandwidth	$V_{O, dm} = 2\text{ V p-p}$	210	240		MHz
Bandwidth for 0.1 dB Flatness	$V_{O, dm} = 0.1\text{ V p-p}$		45		MHz
Slew Rate	$V_{O, dm} = 2\text{ V step}$		800		V/ μs
Settling Time to 0.01%	$V_{O, dm} = 2\text{ V step}$, $C_F = 2\text{ pF}$		45		ns
Overdrive Recovery Time	$G = 2$, $V_{IN, dm} = 12\text{ V p-p}$ triangle wave		30		ns
Noise/Harmonic Performance					
SFDR	$V_{O, dm} = 2\text{ V p-p}$, $f_c = 1\text{ MHz}$		98		dBc
	$V_{O, dm} = 2\text{ V p-p}$, $f_c = 5\text{ MHz}$		85		dBc
	$V_{O, dm} = 2\text{ V p-p}$, $f_c = 20\text{ MHz}$		72		dBc
Third-Order IMD	$V_{O, dm} = 2\text{ V p-p}$, $f_c = 10.05\text{ MHz} \pm 0.05\text{ MHz}$		–90		dBc
Input Voltage Noise	$f = 100\text{ kHz}$		2.25		nV/ $\sqrt{\text{Hz}}$
Input Current Noise	$f = 100\text{ kHz}$		2.1		pA/ $\sqrt{\text{Hz}}$
DC Performance					
Input Offset Voltage	$V_{IP} = V_{IN} = V_{OCM} = 0\text{ V}$	–500	± 150	+500	μV
Input Offset Voltage Drift	T_{MIN} to T_{MAX}		1.25		$\mu\text{V}/^\circ\text{C}$
Input Bias Current	T_{MIN} to T_{MAX}		2.25	8.0	μA
Input Offset Current			0.12	0.5	μA
Open-Loop Gain			114		dB
Input Characteristics					
Input Common-Mode Voltage Range		–4		+4	V
Input Resistance	Differential		600		k Ω
	Common mode		1.5		M Ω
Input Capacitance	Common mode		1.2		pF
CMRR	$\Delta V_{ICM} = \pm 1\text{ V dc}$, $R_F = R_G = 10\text{ k}\Omega$	80	84		dB
Output Characteristics					
Output Voltage Swing	Each single-ended output, $R_F = R_G = 10\text{ k}\Omega$	– $V_S + 0.20$		+ $V_S - 0.20$	V
	Each single-ended output, $R_{L, dm} = \text{open circuit}$, $R_F = R_G = 10\text{ k}\Omega$	– $V_S + 0.15$		+ $V_S - 0.15$	V
Output Current	Each single-ended output		100		mA
Output Balance Error	$f = 1\text{ MHz}$		–69		dB
V_{OCM} TO $V_{O, cm}$ PERFORMANCE					
V_{OCM} Dynamic Performance					
–3 dB Bandwidth	$V_{O, cm} = 0.1\text{ V p-p}$		515		MHz
Slew Rate	$V_{O, cm} = 2\text{ V p-p}$		250		V/ μs
Gain		0.999	1.000	1.001	V/V
V_{OCM} Input Characteristics					
Input Voltage Range		–3.8		+3.8	V
Input Resistance			3.5		M Ω
Input Offset Voltage	$V_{OS, cm} = V_{O, cm} - V_{OCM}$; $V_{IP} = V_{IN} = V_{OCM} = 0\text{ V}$	–900	± 300	+900	μV
Input Voltage Noise	$f = 100\text{ kHz}$		3.5		nV/ $\sqrt{\text{Hz}}$
Input Bias Current			1.3	4.5	μA
CMRR	$\Delta V_{OCM}/\Delta V_{O, dm}$, $\Delta V_{OCM} = \pm 1\text{ V}$	74	88		dB

Parameter	Test Conditions/Comments	Min	Typ	Max	Unit
POWER SUPPLY					
Operating Range		+4.5		±6	V
Quiescent Current			24.5	25.5	mA
+PSRR	Change in $+V_s = \pm 1$ V	95	112		dB
-PSRR	Change in $-V_s = \pm 1$ V	95	109		dB
OPERATING TEMPERATURE RANGE		-40		+125	°C

V_S = 5 V, V_{O,CM} = 2.5 VT_A = 25°C, differential gain = 1, R_{L,dm} = 1 kΩ, R_F = R_G = 200 Ω, unless otherwise noted. T_{MIN} to T_{MAX} = -40°C to +125°C.

Table 2.

Parameter	Test Conditions/Comments	Min	Typ	Max	Unit
DIFFERENTIAL INPUT PERFORMANCE					
Dynamic Performance					
-3 dB Small Signal Bandwidth	V _{O,dm} = 0.1 V p-p	330	385		MHz
-3 dB Large Signal Bandwidth	V _{O,dm} = 2 V p-p	135	165		MHz
Bandwidth for 0.1 dB Flatness	V _{O,dm} = 0.1 V p-p		34		MHz
Slew Rate	V _{O,dm} = 2 V step		540		V/μs
Settling Time to 0.01%	V _{O,dm} = 2 V step		55		ns
Overdrive Recovery Time	G = 2, V _{IN,dm} = 7 V p-p triangle wave		35		ns
Noise/Harmonic Performance					
SFDR	V _{O,dm} = 2 V p-p, f _C = 1 MHz		99		dBc
	V _{O,dm} = 2 V p-p, f _C = 5 MHz, R _L = 800 Ω		87		dBc
	V _{O,dm} = 2 V p-p, f _C = 20 MHz, R _L = 800 Ω		75		dBc
Third-Order IMD	V _{O,dm} = 2 V p-p, f _C = 10.05 MHz ± 0.05 MHz		-87		dBc
Input Voltage Noise	f = 100 kHz		2.25		nV/√Hz
Input Current Noise	f = 100 kHz		2.1		pA/√Hz
DC Performance					
Input Offset Voltage	V _{IP} = V _{IN} = V _{O,CM} = 2.5 V	-500	±150	+500	μV
Input Offset Voltage Drift	T _{MIN} to T _{MAX}		1.25		μV/°C
Input Bias Current	T _{MIN} to T _{MAX}		2.2	7.5	μA
Input Offset Current			0.13	0.5	μA
Open-Loop Gain			112		dB
Input Characteristics					
Input Common-Mode Voltage Range		1		4	V
Input Resistance	Differential		600		kΩ
	Common mode		1.5		MΩ
Input Capacitance	Common mode		1.2		pF
CMRR	ΔV _{ICM} = ±1 V dc, R _F = R _G = 10 kΩ	75	79		dB
Output Characteristics					
Output Voltage Swing	Each single-ended output, R _F = R _G = 10 kΩ	-V _S + 0.15		+V _S - 0.15	V
	Each single-ended output, R _{L,dm} = open circuit, R _F = R _G = 10 kΩ	-V _S + 0.10		+V _S - 0.10	V
Output Current	Each single-ended output		80		mA
Output Balance Error	f = 1 MHz		-70		dB
V_{O,CM} TO V_{O,cm} PERFORMANCE					
V _{O,CM} Dynamic Performance					
-3 dB Bandwidth	V _{O,cm} = 0.1 V p-p		440		MHz
Slew Rate	V _{O,cm} = 2 V p-p		150		V/μs
Gain		0.999	1.000	1.001	V/V
V _{O,CM} Input Characteristics					
Input Voltage Range		1.0		3.8	V
Input Resistance			3.5		MΩ
Input Offset Voltage	V _{OS,cm} = V _{O,cm} - V _{O,CM} ; V _{IP} = V _{IN} = V _{O,CM} = 2.5 V	-1.0	±0.45	+1.0	mV
Input Voltage Noise	f = 100 kHz		3.5		nV/√Hz
Input Bias Current			1.3	4.2	μA
CMRR	ΔV _{O,CM} /ΔV _{O,dm} , ΔV _{O,CM} = ±1 V	67	79		dB

Parameter	Test Conditions/Comments	Min	Typ	Max	Unit
POWER SUPPLY					
Operating Range		+4.5		±6	V
Quiescent Current			21.5	22.5	mA
+PSRR	Change in $+V_s = \pm 1$ V	86	97		dB
-PSRR	Change in $-V_s = \pm 1$ V	92	105		dB
OPERATING TEMPERATURE RANGE		-40		+125	°C

ABSOLUTE MAXIMUM RATINGS

Table 3.

Parameter	Rating
Supply Voltage	12 V
V_{OCM}	$\pm V_S$
Power Dissipation	See Figure 4
Input Common-Mode Voltage	$\pm V_S$
Storage Temperature Range	-65°C to $+125^{\circ}\text{C}$
Operating Temperature Range	-40°C to $+125^{\circ}\text{C}$
Lead Temperature (Soldering 10 sec)	300°C
Junction Temperature	150°C

Stresses at or above those listed under Absolute Maximum Ratings may cause permanent damage to the product. This is a stress rating only; functional operation of the product at these or any other conditions above those indicated in the operational section of this specification is not implied. Operation beyond the maximum operating conditions for extended periods may affect product reliability.

THERMAL RESISTANCE

θ_{JA} is specified for the worst-case conditions, that is, θ_{JA} is specified for device soldered in circuit board for surface-mount packages.

Table 4.

Package Type	θ_{JA}	Unit
8-Lead SOIC with EP/4-Layer	70	$^{\circ}\text{C}/\text{W}$
8-Lead LFCSP/4-Layer	70	$^{\circ}\text{C}/\text{W}$

Maximum Power Dissipation

The maximum safe power dissipation in the AD8139 package is limited by the associated rise in junction temperature (T_J) on the die. At approximately 150°C , which is the glass transition temperature, the plastic changes its properties. Even temporarily exceeding this temperature limit can change the stresses that the package exerts on the die, permanently shifting the parametric performance of the AD8139. Exceeding a junction temperature of 175°C for an extended period can result in changes in the silicon devices potentially causing failure.

The power dissipated in the package (P_D) is the sum of the quiescent power dissipation and the power dissipated in the package due to the load drive for all outputs. The quiescent power is the voltage between the supply pins (V_S) times the quiescent current (I_S). The load current consists of differential and common-mode currents flowing to the load, as well as currents flowing through the external feedback networks and the internal common-mode feedback loop. The internal resistor tap used in the common-mode feedback loop places a $1\text{ k}\Omega$ differential load on the output. RMS output voltages should be considered when dealing with ac signals.

Airflow reduces θ_{JA} . In addition, more metal directly in contact with the package leads from metal traces, through holes, ground, and power planes reduce the θ_{JA} .

Figure 4 shows the maximum safe power dissipation in the package vs. the ambient temperature for the exposed paddle (EP) 8-lead SOIC ($\theta_{JA} = 70^{\circ}\text{C}/\text{W}$) and the 8-lead LFCSP ($\theta_{JA} = 70^{\circ}\text{C}/\text{W}$) on a JEDEC standard 4-layer board. θ_{JA} values are approximations.

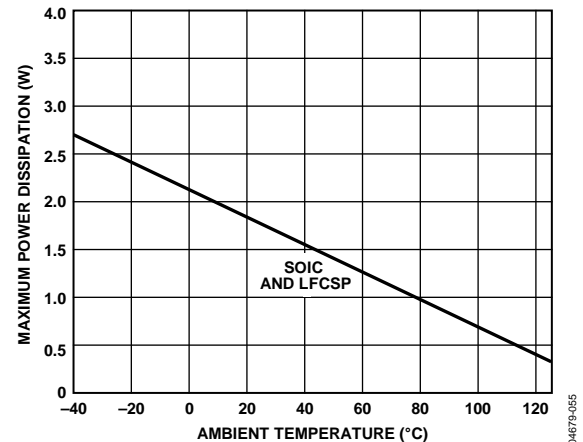


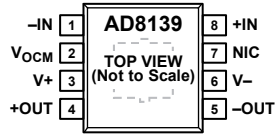
Figure 4. Maximum Power Dissipation vs. Temperature for a 4-Layer Board

ESD CAUTION



ESD (electrostatic discharge) sensitive device. Charged devices and circuit boards can discharge without detection. Although this product features patented or proprietary protection circuitry, damage may occur on devices subjected to high energy ESD. Therefore, proper ESD precautions should be taken to avoid performance degradation or loss of functionality.

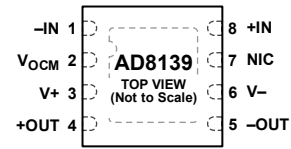
PIN CONFIGURATIONS AND FUNCTION DESCRIPTIONS



NOTES
 1. NIC = NO INTERNAL CONNECTION.
 2. SOLDER THE EXPOSED PADDLE ON THE BACK OF THE PACKAGE TO THE GROUND PLANE OR TO A POWER PLANE.

04679-103

Figure 5. 8-Lead SOIC Pin Configuration



NOTES
 1. NIC = NO INTERNAL CONNECTION.
 2. SOLDER THE EXPOSED PADDLE ON THE BACK OF THE PACKAGE TO THE GROUND PLANE OR TO A POWER PLANE.

04679-103

Figure 6. 8-Lead LFCSP Pin Configuration

Table 5. Pin Function Descriptions

Pin No.	Mnemonic	Description
1	-IN	Inverting Input.
2	V _{OCM}	An internal feedback loop drives the output common-mode voltage to be equal to the voltage applied to the V _{OCM} pin, provided the operation of the amplifier remains linear.
3	V+	Positive Power Supply Voltage.
4	+OUT	Positive Side of the Differential Output.
5	-OUT	Negative Side of the Differential Output.
6	V-	Negative Power Supply Voltage.
7	NIC	No Internal Connection.
8	+IN	Noninverting Input.
0	EP	Exposed Paddle. Solder the exposed paddle on the back of the package to the ground plane or to a power plane.

TYPICAL PERFORMANCE CHARACTERISTICS

Unless otherwise noted, differential gain = +1, $R_G = R_F = 200 \Omega$, $R_{L, dm} = 1 \text{ k}\Omega$, $V_S = \pm 5 \text{ V}$, $T_A = 25^\circ\text{C}$, $V_{OCM} = 0 \text{ V}$. Refer to the basic test circuit in Figure 57 for the definition of terms.

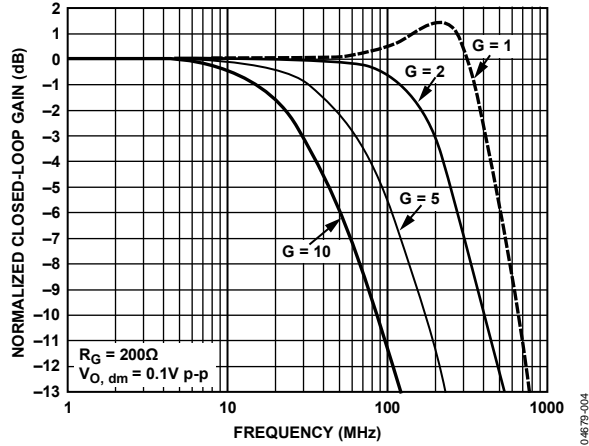


Figure 7. Small Signal Frequency Response for Various Gains

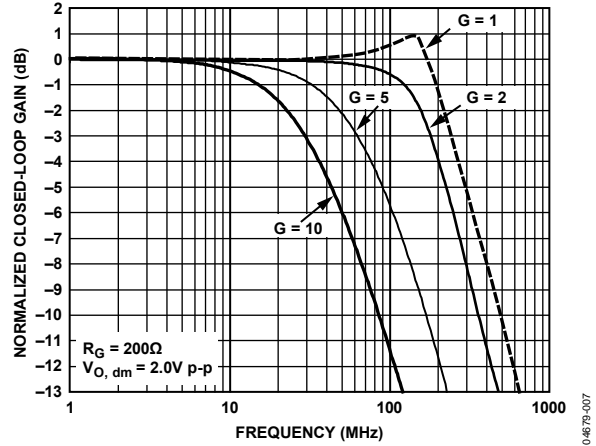


Figure 10. Large Signal Frequency Response for Various Gains

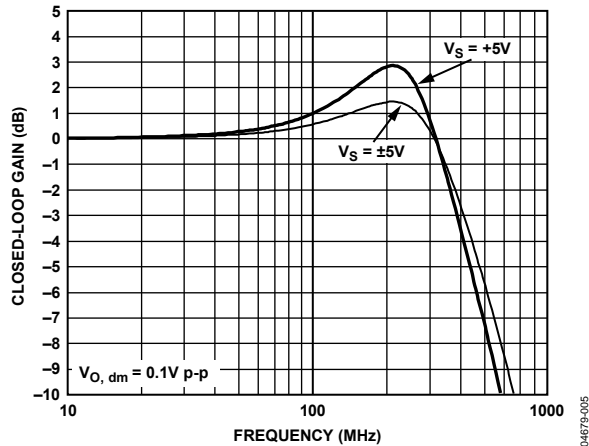


Figure 8. Small Signal Frequency Response for Various Power Supplies

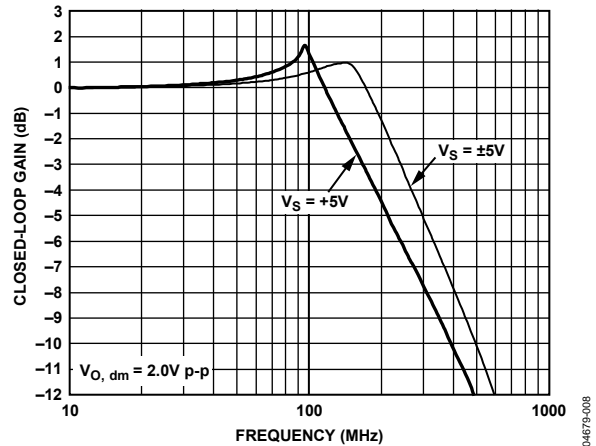


Figure 11. Large Signal Frequency Response for Various Power Supplies

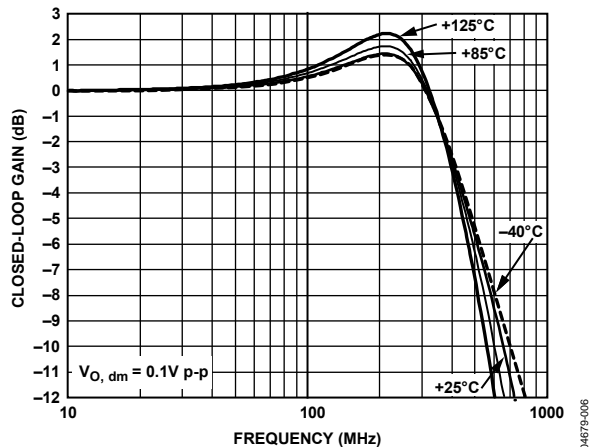


Figure 9. Small Signal Frequency Response at Various Temperatures

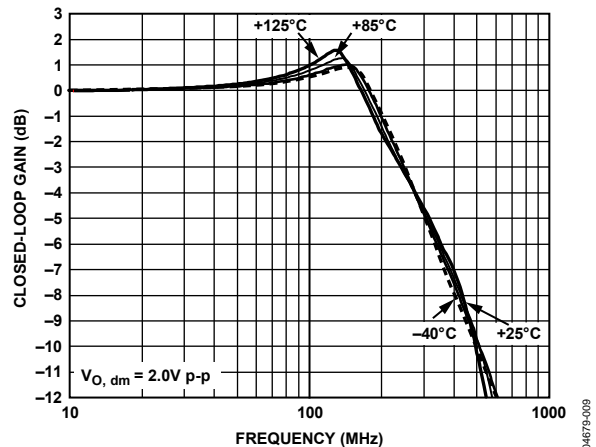


Figure 12. Large Signal Frequency Response at Various Temperatures

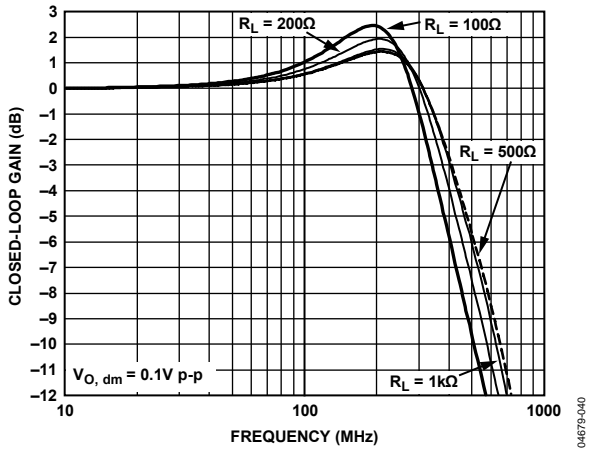


Figure 13. Small Signal Frequency Response for Various Loads

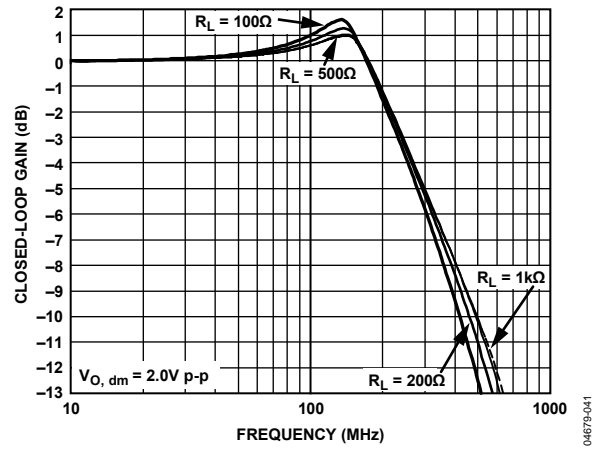


Figure 16. Large Signal Frequency Response for Various Loads

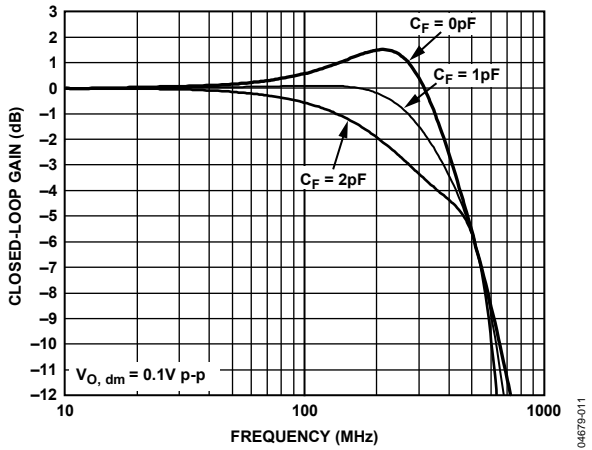


Figure 14. Small Signal Frequency Response for Various C_F

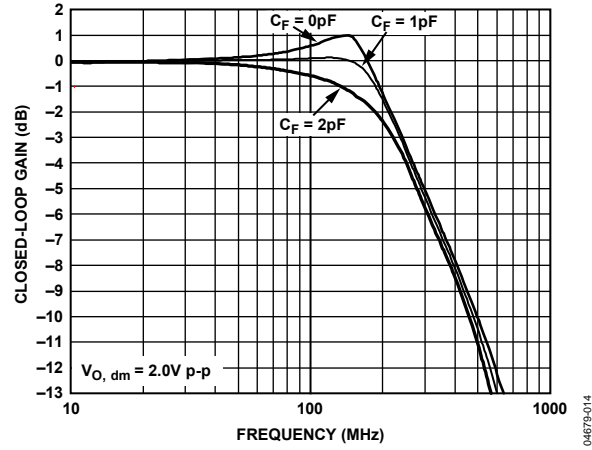


Figure 17. Large Signal Frequency Response for Various C_F

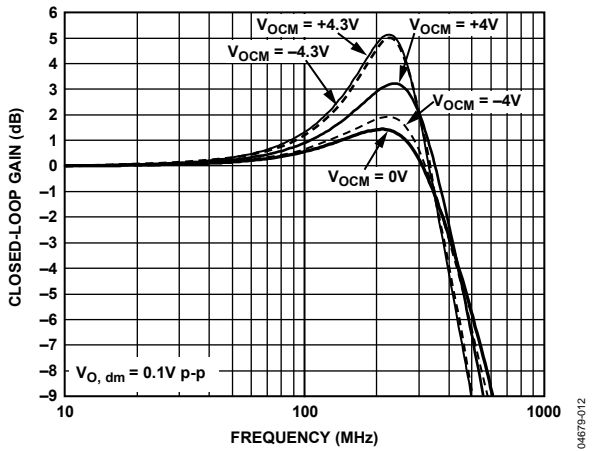


Figure 15. Small Signal Frequency Response at Various V_{OCM}

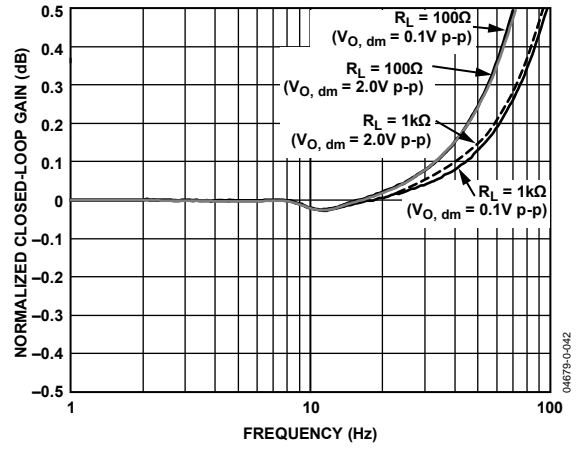


Figure 18. 0.1 dB Flatness for Various Loads and Output Amplitudes

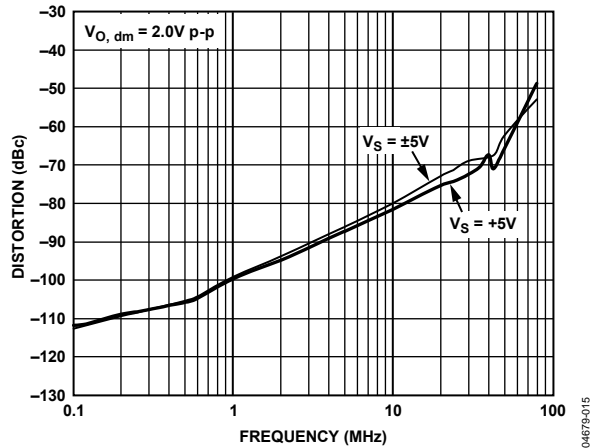


Figure 19. Second Harmonic Distortion vs. Frequency and Supply Voltage

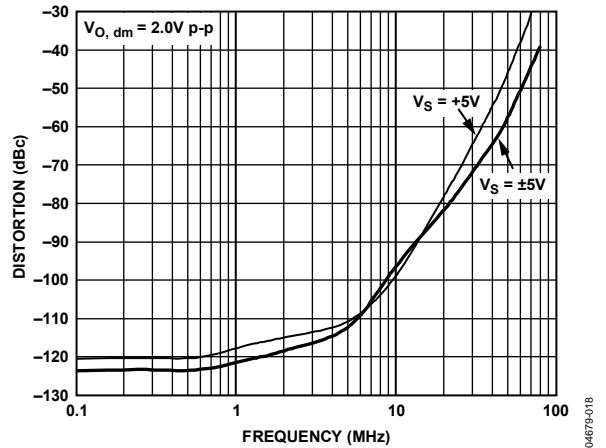


Figure 22. Third Harmonic Distortion vs. Frequency and Supply Voltage

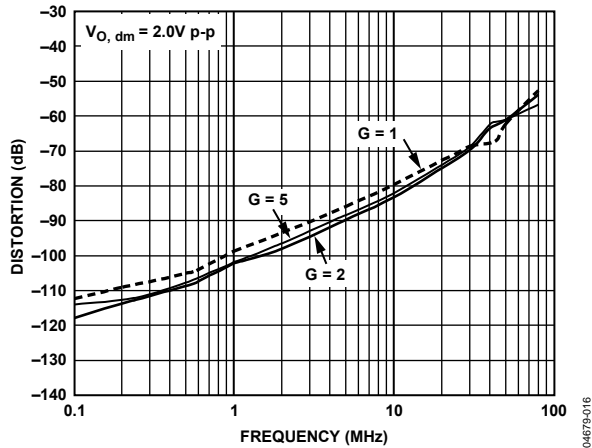


Figure 20. Second Harmonic Distortion vs. Frequency and Gain

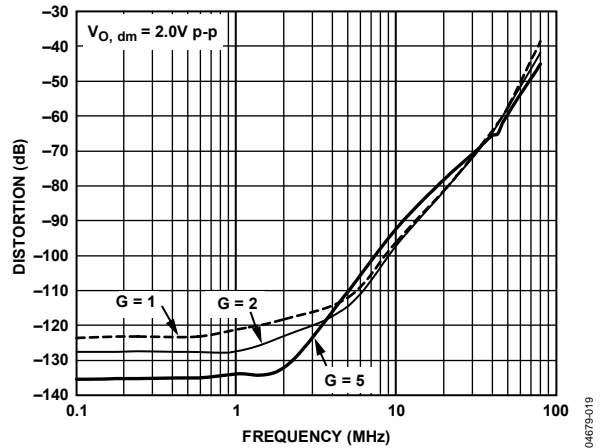


Figure 23. Third Harmonic Distortion vs. Frequency and Gain

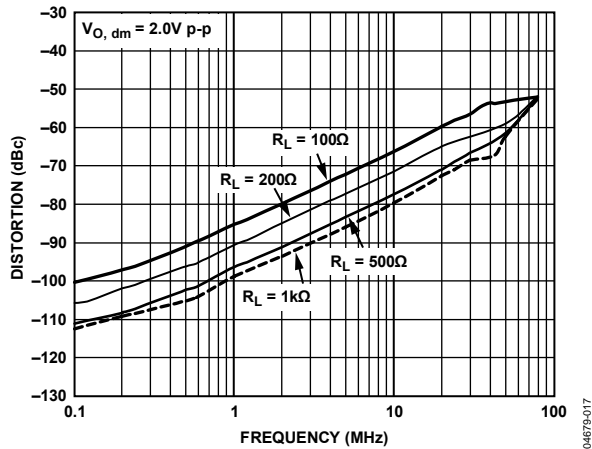


Figure 21. Second Harmonic Distortion vs. Frequency and Load

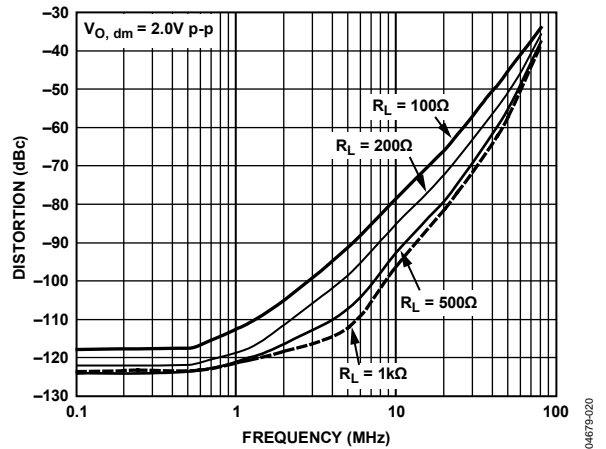


Figure 24. Third Harmonic Distortion vs. Frequency and Load

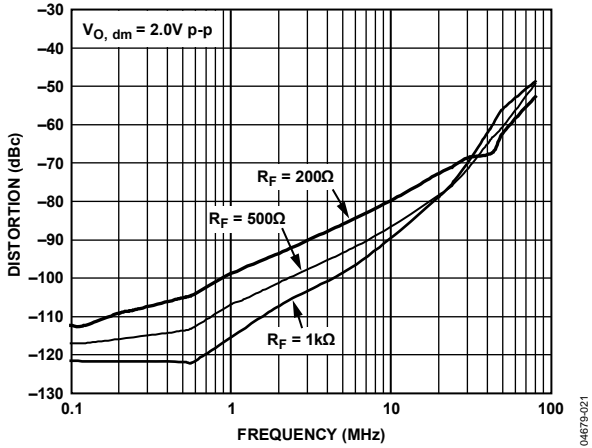


Figure 25. Second Harmonic Distortion vs. Frequency and R_F

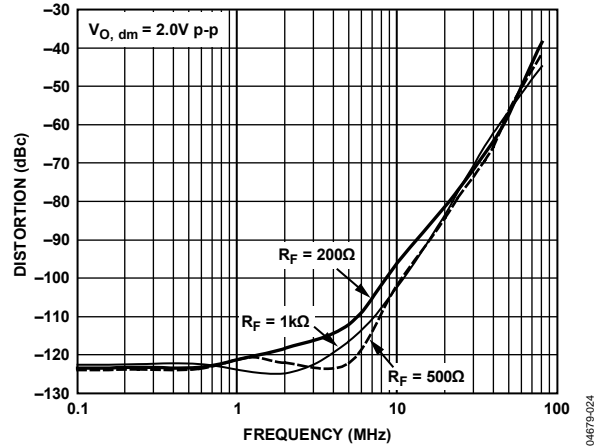


Figure 28. Third Harmonic Distortion vs. Frequency and R_F

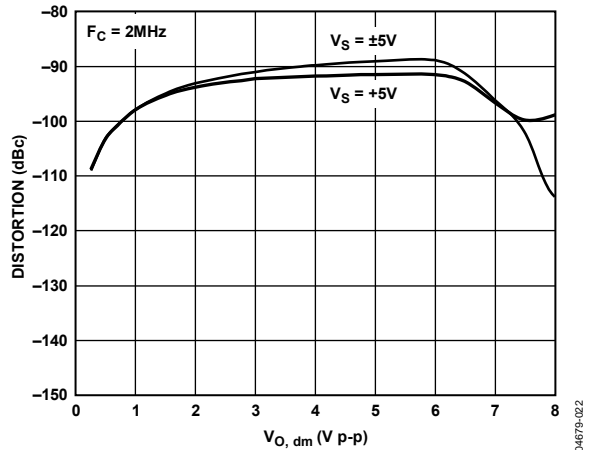


Figure 26. Second Harmonic Distortion vs. Output Amplitude

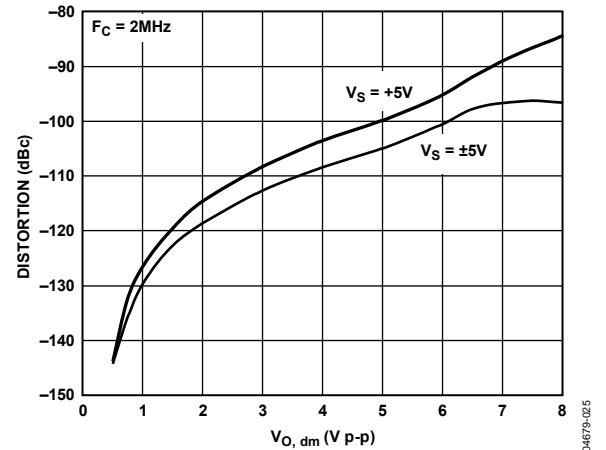


Figure 29. Third Harmonic Distortion vs. Output Amplitude

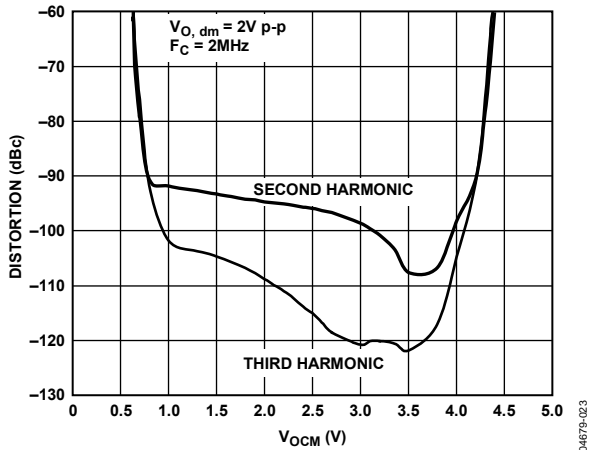


Figure 27. Harmonic Distortion vs. V_{OCM} , $V_S = +5V$

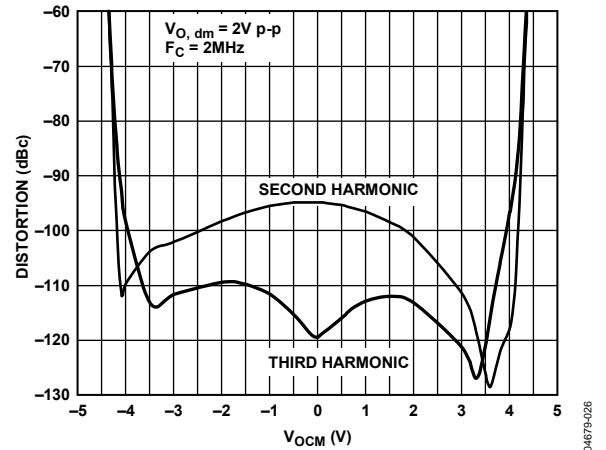


Figure 30. Harmonic Distortion vs. V_{OCM} , $V_S = \pm 5V$

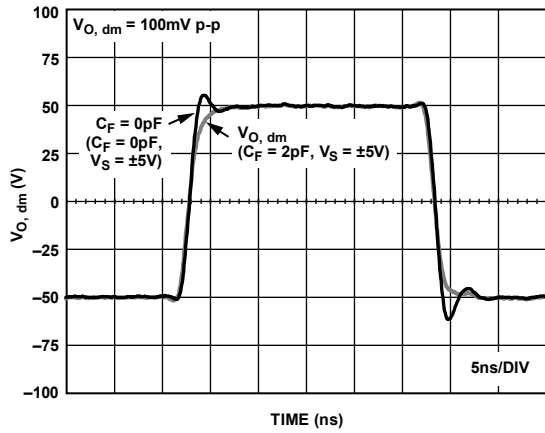


Figure 31. Small Signal Transient Response for Various C_f

04679-043

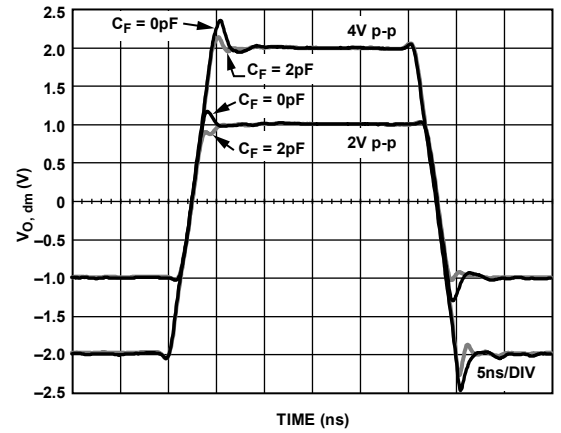


Figure 34. Large Signal Transient Response for Various C_f

04679-044

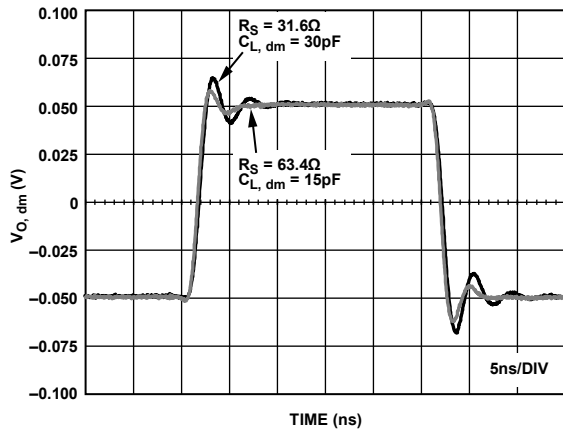


Figure 32. Small Signal Transient Response for Capacitive Loads

04679-064

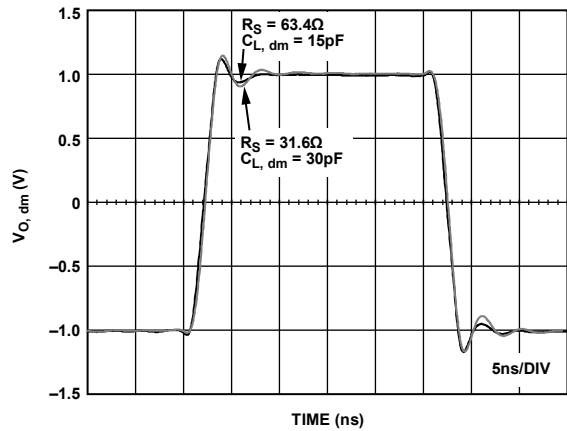


Figure 35. Large Signal Transient Response for Capacitive Loads

04679-065

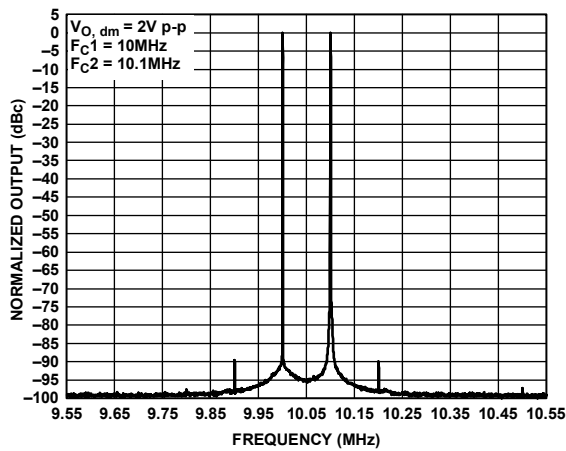


Figure 33. Intermodulation Distortion

04679-027

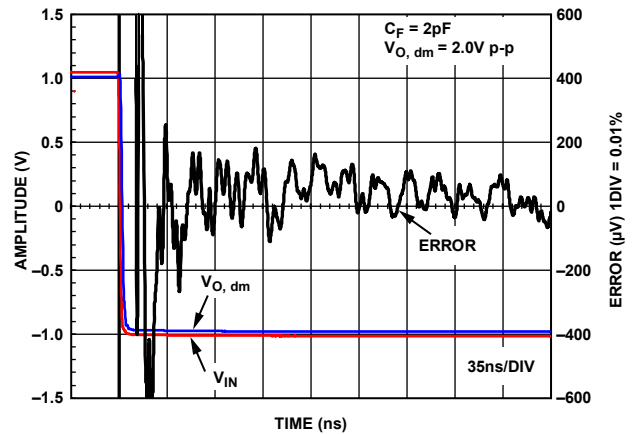


Figure 36. Settling Time (0.01%)

04679-034

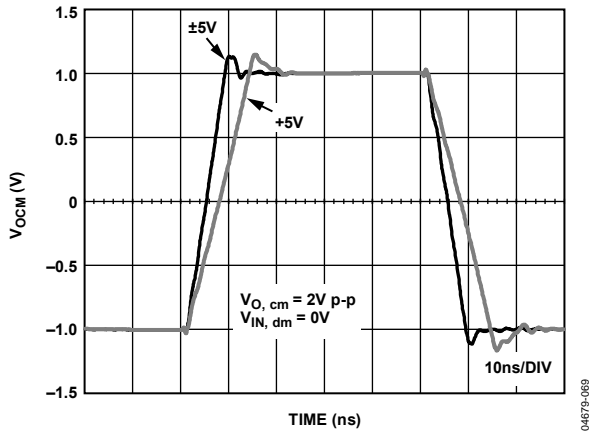


Figure 37. V_{OCM} Large Signal Transient Response

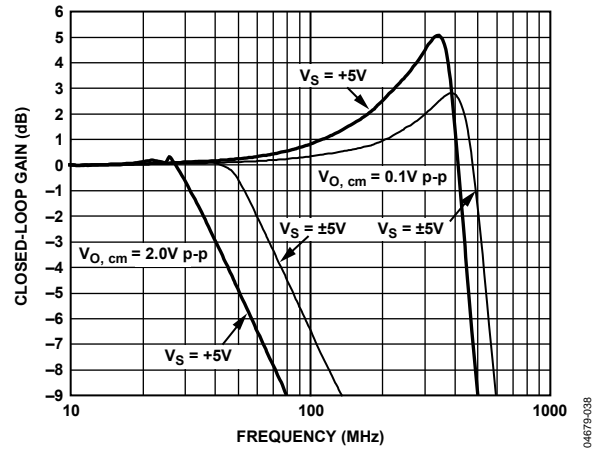


Figure 40. V_{OCM} Frequency Response for Various Supplies

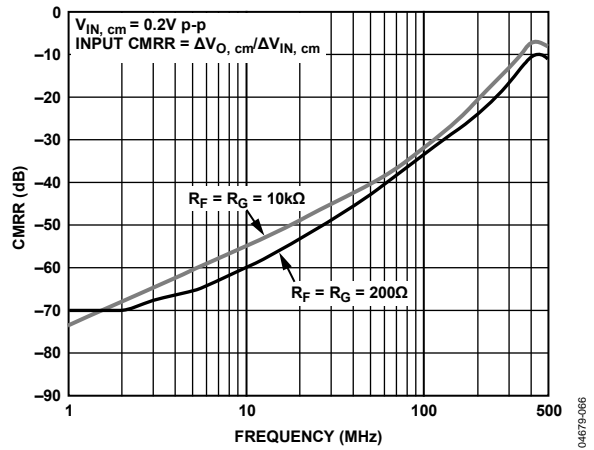


Figure 38. CMRR vs. Frequency

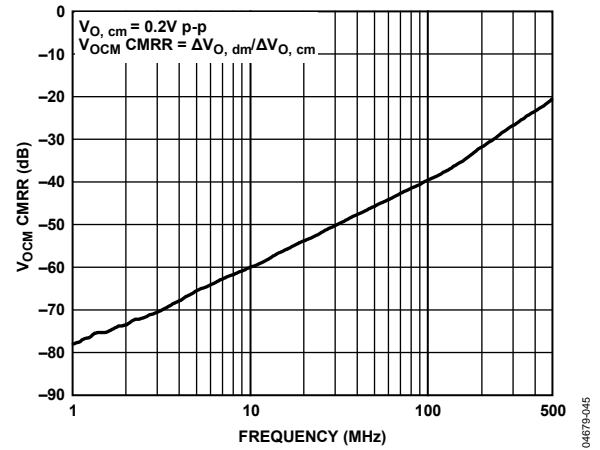


Figure 41. V_{OCM} CMRR vs. Frequency

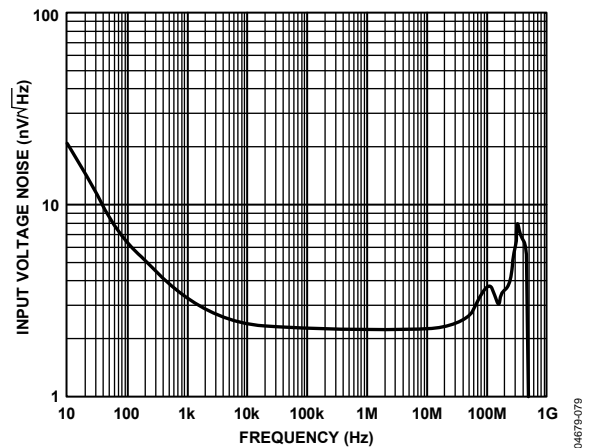


Figure 39. Input Voltage Noise vs. Frequency

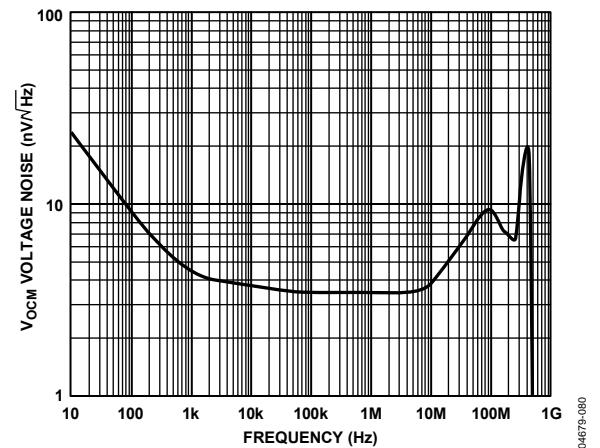


Figure 42. V_{OCM} Voltage Noise vs. Frequency

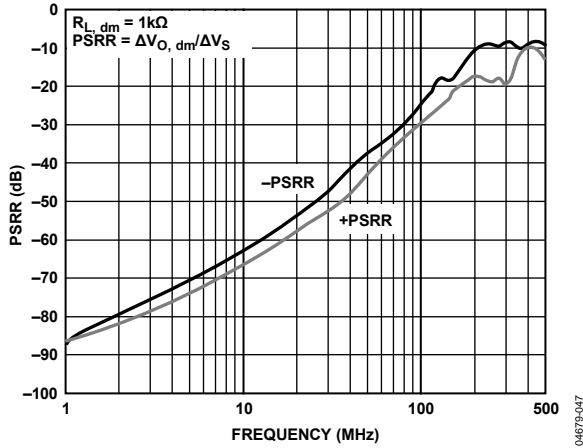


Figure 43. PSRR vs. Frequency

04679-047

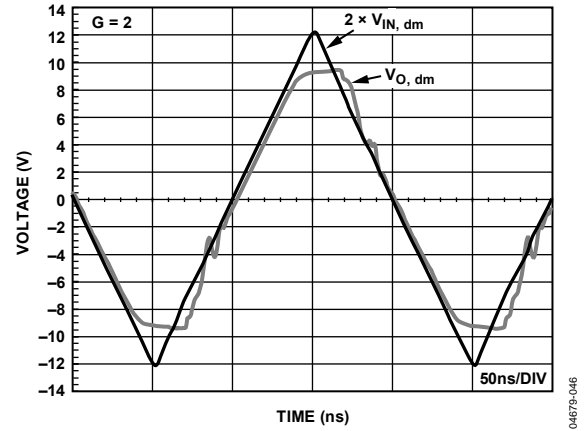


Figure 46. Overdrive Recovery

04679-046

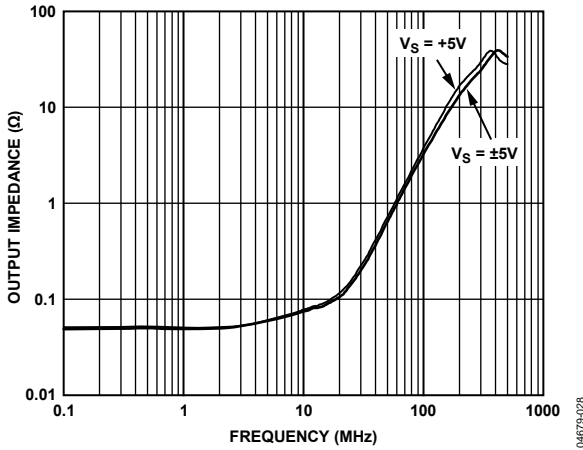


Figure 44. Single-Ended Output Impedance vs. Frequency

04679-028

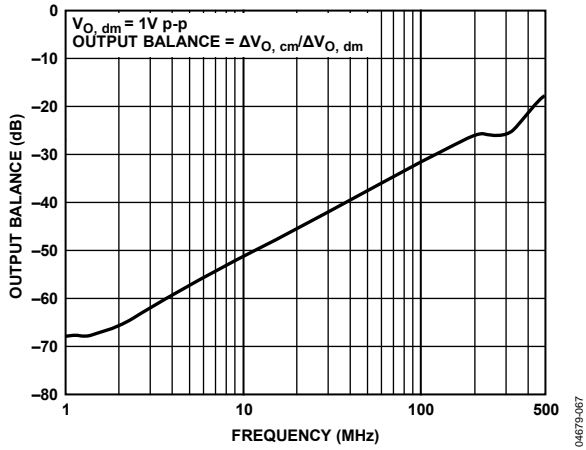


Figure 47. Output Balance vs. Frequency

04679-067

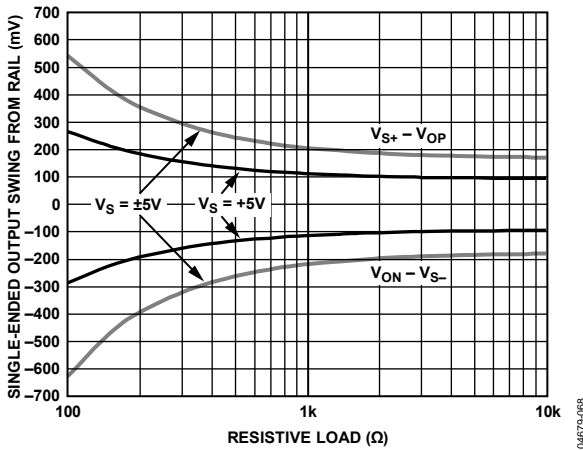


Figure 45. Output Saturation Voltage vs. Output Load

04679-065

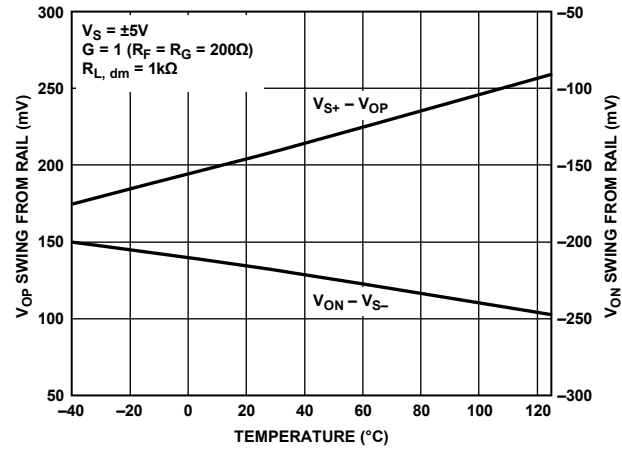


Figure 48. Output Saturation Voltage vs. Temperature

04679-077

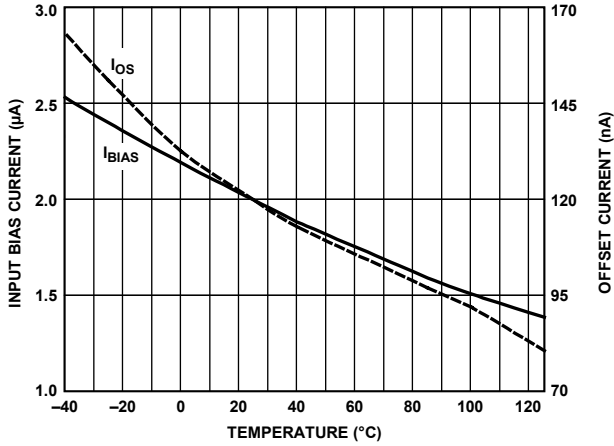


Figure 49. Input Bias and Offset Current vs. Temperature

04679-062

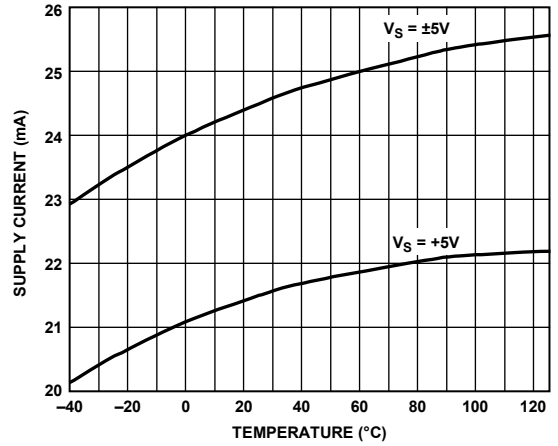


Figure 52. Supply Current vs. Temperature

04679-060

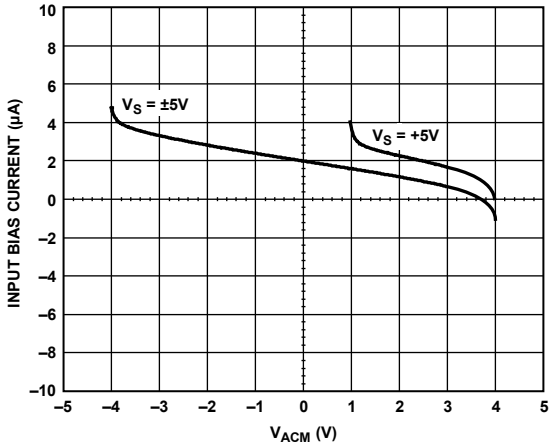


Figure 50. Input Bias Current vs. Input Common-Mode Voltage

04679-073

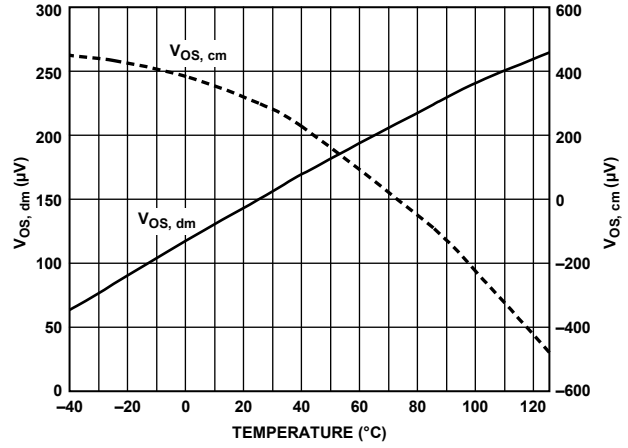


Figure 53. Offset Voltage vs. Temperature

04679-061

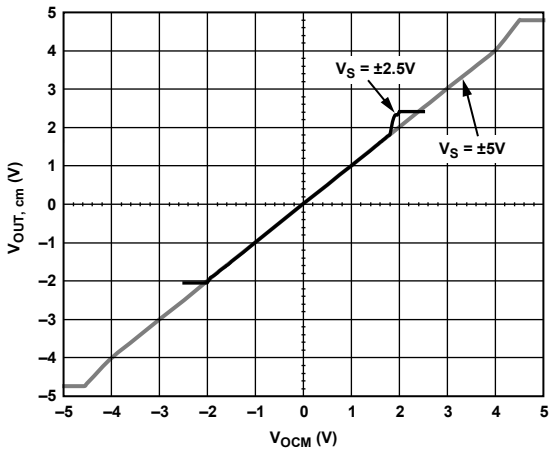


Figure 51. $V_{OUT, cm}$ vs. V_{OCM} Input Voltage

04679-048

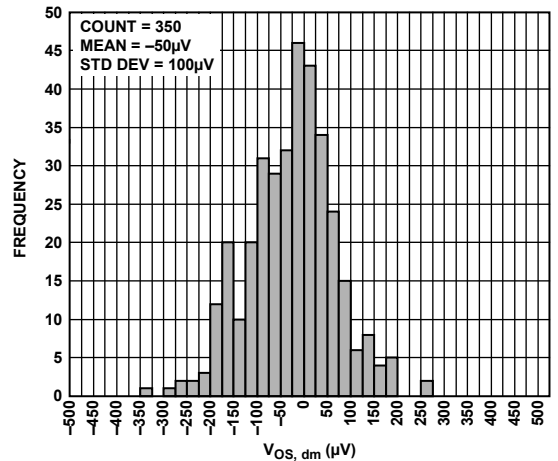


Figure 54. $V_{OS, dm}$ Distribution

04679-071

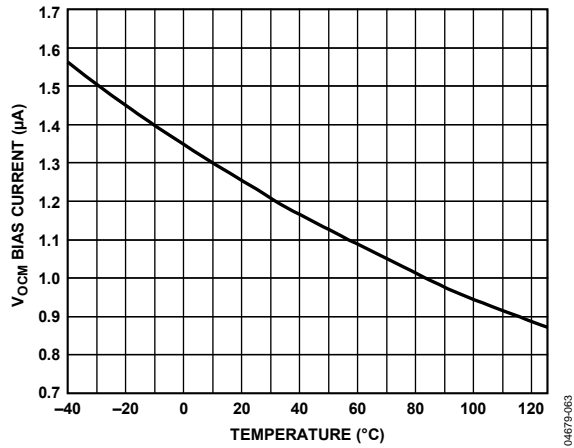


Figure 55. Vocm Bias Current vs. Temperature

04679-083

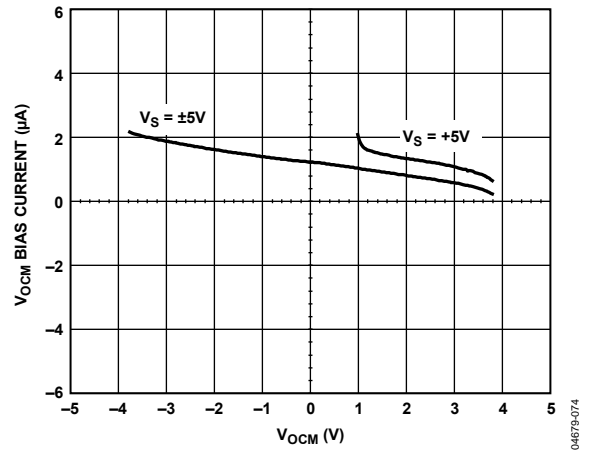


Figure 56. Vocm Bias Current vs. Vocm Input Voltage

04679-074

TEST CIRCUITS

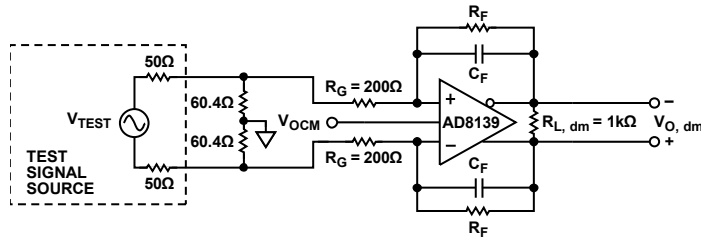


Figure 57. Basic Test Circuit

04679-072

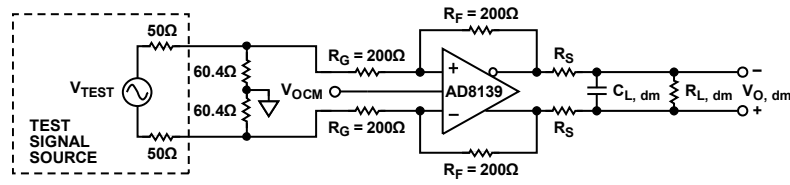


Figure 58. Capacitive Load Test Circuit, $G = +1$

04679-075

THEORY OF OPERATION

The AD8139 is a high speed, low noise differential amplifier fabricated on the Analog Devices second-generation extra fast complementary bipolar (XFCEB) process. It is designed to provide two closely balanced differential outputs in response to either differential or single-ended input signals. Differential gain is set by external resistors, similar to traditional voltage-feedback operational amplifiers. The common-mode level of the output voltage is set by a voltage at the V_{OCM} pin and is independent of the input common-mode voltage. The AD8139 has an H-bridge input stage for high slew rate, low noise, and low distortion operation and rail-to-rail output stages that provide maximum dynamic output range. This set of features allows for convenient single-ended-to-differential conversion, a common need to take advantage of modern high resolution ADCs with differential inputs.

TYPICAL CONNECTION AND DEFINITION OF TERMS

Figure 59 shows a typical connection for the AD8139, using matched external R_F/R_G networks. The differential input terminals of the AD8139, V_{AP} and V_{AN} , are used as summing junctions. An external reference voltage applied to the V_{OCM} terminal sets the output common-mode voltage. The two output terminals, V_{OP} and V_{ON} , move in opposite directions in a balanced fashion in response to an input signal.

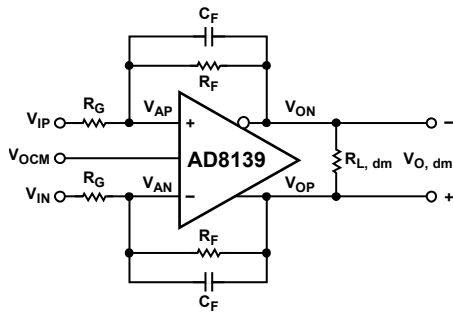


Figure 59. Typical Connection

The differential output voltage is defined as

$$V_{O, dm} = V_{OP} - V_{ON} \tag{1}$$

Common-mode voltage is the average of two voltages. The output common-mode voltage is defined as

$$V_{O, cm} = \frac{V_{OP} + V_{ON}}{2} \tag{2}$$

Output Balance

Output balance is a measure of how well V_{OP} and V_{ON} are matched in amplitude and how precisely they are 180° out of phase with each other. It is the internal common-mode feedback loop that forces the signal component of the output common-mode towards zero, resulting in the near perfectly balanced differential

outputs of identical amplitude and exactly 180° out of phase. The output balance performance does not require tightly matched external components, nor does it require that the feedback factors of each loop be equal to each other. Low frequency output balance is limited ultimately by the mismatch of an on-chip voltage divider, which is trimmed for optimum performance.

Output balance is measured by placing a well-matched resistor divider across the differential voltage outputs and comparing the signal at the midpoint of the divider with the magnitude of the differential output. By this definition, output balance is equal to the magnitude of the change in output common-mode voltage divided by the magnitude of the change in output differential-mode voltage:

$$\text{Output Balance} = \left| \frac{\Delta V_{O, cm}}{\Delta V_{O, dm}} \right| \tag{3}$$

The block diagram of the AD8139 in Figure 60 shows the external differential feedback loop (R_F/R_G networks and the differential input transconductance amplifier, G_{DIFF}) and the internal common-mode feedback loop (voltage divider across V_{OP} and V_{ON} and the common-mode input transconductance amplifier, G_{CM}). The differential negative feedback drives the voltages at the summing junctions V_{AN} and V_{AP} to be essentially equal to each other.

$$V_{AN} = V_{AP} \tag{4}$$

The common-mode feedback loop drives the output common-mode voltage, sampled at the midpoint of the two 500 Ω resistors, to equal the voltage set at the V_{OCM} terminal. This ensures that

$$V_{OP} = V_{OCM} + \frac{V_{O, dm}}{2} \tag{5}$$

and

$$V_{ON} = V_{OCM} - \frac{V_{O, dm}}{2} \tag{6}$$

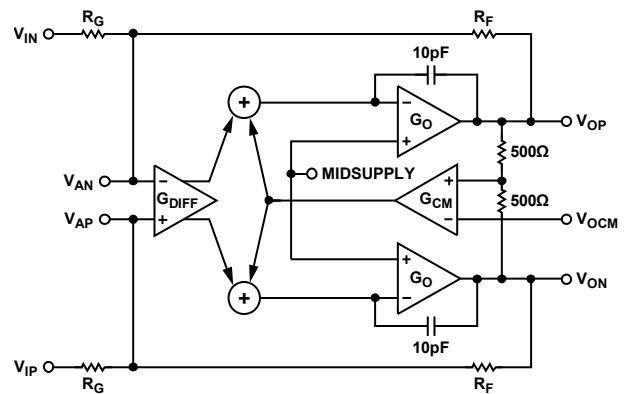


Figure 60. Block Diagram

APPLICATIONS INFORMATION

ESTIMATING NOISE, GAIN, AND BANDWIDTH WITH MATCHED FEEDBACK NETWORKS

Estimating Output Noise Voltage

The total output noise is calculated as the root-sum-squared total of several statistically independent sources. Because the sources are statistically independent, the contributions of each must be individually included in the root-sum-square calculation. Table 6 lists recommended resistor values and estimates of bandwidth and output differential voltage noise for various closed-loop gains. For most applications, 1% resistors are sufficient.

Table 6. Recommended Values of Gain-Setting Resistors and Voltage Noise for Various Closed-Loop Gains

Gain	R _G (Ω)	R _F (Ω)	3 dB Bandwidth (MHz)	Total Output Noise (nV/√Hz)
1	200	200	400	5.8
2	200	400	160	9.3
5	200	1 k	53	19.7
10	200	2 k	26	37

The differential output voltage noise contains contributions from the input voltage noise and input current noise of the AD8139 as well as those from the external feedback networks.

The contribution from the input voltage noise spectral density is computed as

$$V_{o_n1} = v_n \left(1 + \frac{R_F}{R_G} \right), \text{ or equivalently, } v_n/\beta \quad (7)$$

where v_n is defined as the input-referred differential voltage noise. This equation is the same as that of traditional op amps.

The contribution from the input current noise of each input is computed as

$$V_{o_n2} = i_n (R_F) \quad (8)$$

where i_n is defined as the input noise current of one input. Each input needs to be treated separately because the two input currents are statistically independent processes.

The contribution from each R_G is computed as

$$V_{o_n3} = \sqrt{4kTR_G} \left(\frac{R_F}{R_G} \right) \quad (9)$$

This result can be intuitively viewed as the thermal noise of each R_G multiplied by the magnitude of the differential gain.

The contribution from each R_F is computed as

$$V_{o_n4} = \sqrt{4kTR_F} \quad (10)$$

Voltage Gain

The behavior of the node voltages of the single-ended-to-differential output topology can be deduced from the previous definitions. Referring to Figure 59, ($C_F = 0$) and setting $V_{IN} = 0$, one can write

$$\frac{V_{IP} - V_{AP}}{R_G} = \frac{V_{AP} - V_{ON}}{R_F} \quad (11)$$

$$V_{AN} = V_{AP} = V_{OP} \left(\frac{R_G}{R_F + R_G} \right) \quad (12)$$

Solving the above two equations and setting V_{IP} to V_i gives the gain relationship for $V_{O, dm}/V_i$.

$$V_{OP} - V_{ON} = V_{O, dm} = \frac{R_F}{R_G} V_i \quad (13)$$

An inverting configuration with the same gain magnitude can be implemented by simply applying the input signal to V_{IN} and setting $V_{IP} = 0$. For a balanced differential input, the gain from $V_{IN, dm}$ to $V_{O, dm}$ is also equal to R_F/R_G , where $V_{IN, dm} = V_{IP} - V_{IN}$.

Feedback Factor Notation

When working with differential amplifiers, it is convenient to introduce the feedback factor β , which is defined as

$$\beta = \frac{R_G}{R_F + R_G} \quad (14)$$

This notation is consistent with conventional feedback analysis and is very useful, particularly when the two feedback loops are not matched.

Input Common-Mode Voltage

The linear range of the V_{AN} and V_{AP} terminals extends to within approximately 1 V of either supply rail. Because V_{AN} and V_{AP} are essentially equal to each other, they are both equal to the input common-mode voltage of the amplifier. Their range is indicated in the Specifications tables as input common-mode range. The voltage at V_{AN} and V_{AP} for the connection diagram in Figure 59 can be expressed as

$$V_{AN} = V_{AP} = V_{ACM} = \left(\frac{R_F}{R_F + R_G} \times \frac{(V_{IP} + V_{IN})}{2} \right) + \left(\frac{R_G}{R_F + R_G} \times V_{OCM} \right) \quad (15)$$

where V_{ACM} is the common-mode voltage present at the amplifier input terminals.

Using the β notation, Equation 15 can be written as follows:

$$V_{ACM} = \beta V_{OCM} + (1 - \beta) V_{ICM} \quad (16)$$

or equivalently,

$$V_{ACM} = V_{ICM} + \beta(V_{OCM} - V_{ICM}) \quad (17)$$

where V_{ICM} is the common-mode voltage of the input signal, that is, $V_{ICM} = V_{IP} + V_{IN}/2$.

For proper operation, the voltages at V_{AN} and V_{AP} must stay within their respective linear ranges.

Calculating Input Impedance

The input impedance of the circuit in Figure 59 depends on whether the amplifier is being driven by a single-ended or a differential signal source. For balanced differential input signals, the differential input impedance ($R_{IN, dm}$) is simply

$$R_{IN, dm} = 2R_G \tag{18}$$

For a single-ended signal (for example, when V_{IN} is grounded and the input signal drives V_{IP}), the input impedance becomes

$$R_{IN} = \frac{R_G}{1 - \frac{R_G}{R_F}} \tag{19}$$

The input impedance of a conventional inverting op amp configuration is simply R_G , but it is higher in Equation 19 because a fraction of the differential output voltage appears at the summing junctions, V_{AN} and V_{AP} . This voltage partially bootstraps the voltage across the input resistor R_G , leading to the increased input resistance.

Input Common-Mode Swing Considerations

In some single-ended-to-differential applications, when using a single-supply voltage, attention must be paid to the swing of the input common-mode voltage, V_{ACM} .

Consider the case in Figure 61, where V_{IN} is 5 V p-p swinging about a baseline at ground, and V_{REF} is connected to ground.

The circuit has a differential gain of 1.6 and $\beta = 0.38$. V_{ICM} has an amplitude of 2.5 V p-p and is swinging about ground. Using the results in Equation 16, the common-mode voltage at the inputs of the AD8139, V_{ACM} , is a 1.5 V p-p signal swinging about a baseline of 0.95 V. The maximum negative excursion of V_{ACM} in this case is 0.2 V, which exceeds the lower input common-mode voltage limit.

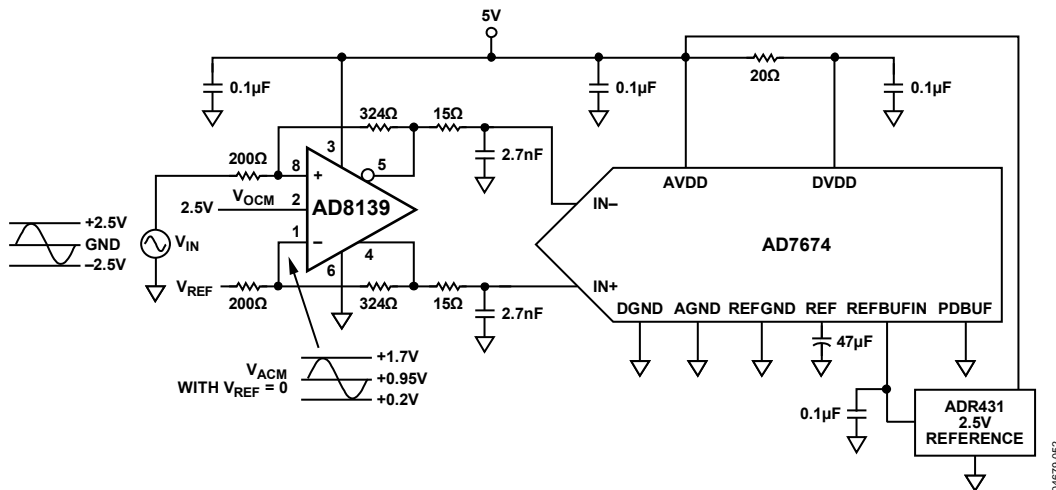


Figure 61. AD8139 Driving AD7674, 18-Bit, 800 kSPS ADC

One way to avoid the input common-mode swing limitation is to bias V_{IN} and V_{REF} at midsupply. In this case, V_{IN} is 5 V p-p swinging about a baseline at 2.5 V, and V_{REF} is connected to a low-Z 2.5 V source. V_{ICM} now has an amplitude of 2.5 V p-p and is swinging about 2.5 V. Using the results in Equation 17, V_{ACM} is calculated to be equal to V_{ICM} because $V_{OCM} = V_{ICM}$. Therefore, V_{ACM} swings from 1.25 V to 3.75 V, which is well within the input common-mode voltage limits of the AD8139. Another benefit seen in this example is that because $V_{OCM} = V_{ACM} = V_{ICM}$ no wasted common-mode current flows. Figure 62 illustrates how to provide the low-Z bias voltage. For situations that do not require a precise reference, a simple voltage divider suffices to develop the input voltage to the buffer.

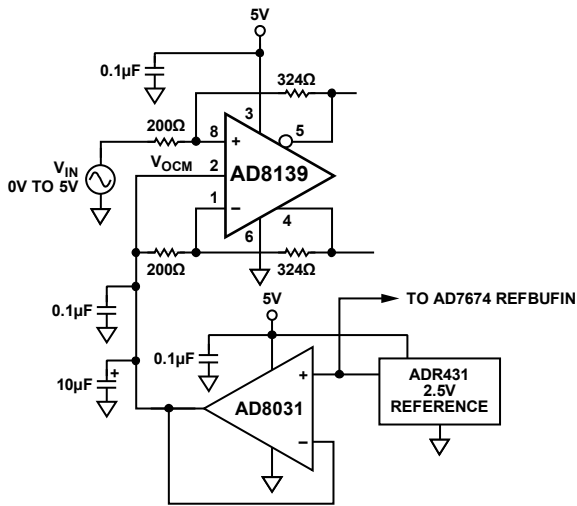


Figure 62. Low-Z 2.5 V Buffer

Another way to avoid the input common-mode swing limitation is to use dual power supplies on the AD8139. In this case, the biasing circuitry is not required.

Bandwidth vs. Closed-Loop Gain

The 3 dB bandwidth of the AD8139 decreases proportionally to increasing closed-loop gain in the same way as a traditional voltage feedback operational amplifier. For closed-loop gains greater than 4, the bandwidth obtained for a specific gain can be estimated as

$$f - 3 \text{ dB}, V_{OUT, dm} = \frac{R_G}{R_G + R_F} \times (300 \text{ MHz}) \quad (20)$$

or equivalently, $\beta(300 \text{ MHz})$.

This estimate assumes a minimum 90° phase margin for the amplifier loop, which is a condition approached for gains greater than 4. Lower gains show more bandwidth than predicted by the equation due to the peaking produced by the lower phase margin.

Estimating DC Errors

Primary differential output offset errors in the AD8139 are due to three major components: the input offset voltage, the offset between the V_{AN} and V_{AP} input currents interacting with the feedback network resistances, and the offset produced by the dc voltage difference between the input and output common-mode voltages in conjunction with matching errors in the feedback network.

The first output error component is calculated as

$$V_{O_e1} = V_{IO} \left(\frac{R_F + R_G}{R_G} \right), \text{ or equivalently as } V_{IO}/\beta \quad (21)$$

where V_{IO} is the input offset voltage. The input offset voltage of the AD8139 is laser trimmed and guaranteed to be less than 500 μV .

The second error is calculated as

$$V_{O_e2} = I_{IO} \left(\frac{R_F + R_G}{R_G} \right) \left(\frac{R_G R_F}{R_F + R_G} \right) = I_{IO} (R_F) \quad (22)$$

where I_{IO} is defined as the offset between the two input bias currents.

The third error voltage is calculated as

$$V_{O_e3} = \Delta nr \times (V_{ICM} - V_{OCM}) \quad (23)$$

where Δnr is the fractional mismatch between the two feedback resistors.

The total differential offset error is the sum of these three error sources.

Other Impact of Mismatches in the Feedback Networks

The internal common-mode feedback network still forces the output voltages to remain balanced, even when the R_F/R_G feedback networks are mismatched. However, the mismatch causes a gain error proportional to the feedback network mismatch.

Ratio-matching errors in the external resistors degrade the ability to reject common-mode signals at the V_{AN} and V_{IN} input terminals, much the same as with a four-resistor difference amplifier made from a conventional op amp. Ratio-matching errors also produce a differential output component that is equal to the V_{OCM} input voltage times the difference between the feedback factors (β s). In most applications using 1% resistors, this component amounts to a differential dc offset at the output that is small enough to be ignored.

Driving a Capacitive Load

A purely capacitive load reacts with the bondwire and pin inductance of the AD8139, resulting in high frequency ringing in the transient response and loss of phase margin. One way to minimize this effect is to place a small resistor in series with each output to buffer the load capacitance (see Figure 58 and Figure 63). The resistor and load capacitance form a first-order, low-pass filter; therefore, the resistor value should be as small as possible. In some cases, the ADCs require small series resistors to be added on their inputs.

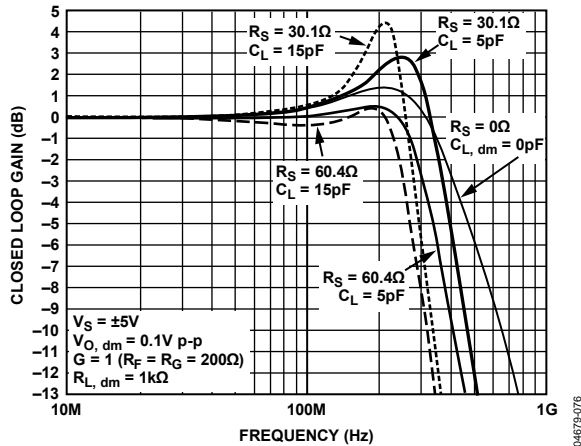


Figure 63. Frequency Response for Various Capacitive Loads and Series Resistances

The Typical Performance Characteristics that illustrate transient response vs. the capacitive load were generated using series resistors in each output and a differential capacitive load.

Layout Considerations

Standard high speed PCB layout practices should be adhered to when designing with the AD8139. A solid ground plane is recommended, and good wideband power supply decoupling networks should be placed as close as possible to the supply pins.

To minimize stray capacitance at the summing nodes, the copper in all layers under all traces and pads that connect to the summing nodes should be removed. Small amounts of stray summing-node capacitance cause peaking in the frequency response, and large amounts can cause instability. If some stray summing-node capacitance is unavoidable, its effects can be compensated for by placing small capacitors across the feedback resistors.

Terminating a Single-Ended Input

Controlled impedance interconnections are used in most high speed signal applications, and they require at least one line termination. In analog applications, a matched resistive termination is generally placed at the load end of the line. This section deals with how to properly terminate a single-ended input to the AD8139.

The input resistance presented by the AD8139 input circuitry is seen in parallel with the termination resistor, and its loading effect must be taken into account. The Thevenin equivalent circuit of the driver, its source resistance, and the termination resistance must all be included in the calculation as well. An exact solution to the problem requires the solution of several simultaneous algebraic equations and is beyond the scope of this data sheet. An iterative solution is also possible and simpler, especially considering the fact that standard 1% resistor values are generally used.

Figure 64 shows the AD8139 in a unity-gain configuration driving the AD6645, which is a 14-bit, high speed ADC, and with the following discussion, provides a good example of how to provide a proper termination in a 50 Ω environment.

The termination resistor, R_T , in parallel with the 268 Ω input resistance of the AD8139 circuit (calculated using Equation 19), yields an overall input resistance of 50 Ω that is seen by the signal source. To have matched feedback loops, each loop must have the same R_G if they have the same R_F . In the input (upper) loop, R_G is equal to the 200 Ω resistor in series with the (+) input plus the parallel combination of R_T and the source resistance of 50 Ω . In the upper loop, R_G is therefore equal to 228 Ω . The closest standard 1% value to 228 Ω is 226 Ω and is used for R_G in the lower loop. Greater accuracy could be achieved by using two resistors in series to obtain a resistance closer to 228 Ω .

Things get more complicated when it comes to determining the feedback resistor values. The amplitude of the signal source generator V_S is two times the amplitude of its output signal when terminated in 50 Ω . Therefore, a 2 V p-p terminated amplitude is produced by a 4 V p-p amplitude from V_S . The Thevenin equivalent circuit of the signal source and R_T must be used when calculating the closed-loop gain, because in the upper loop, R_G is split between the 200 Ω resistor and the Thevenin resistance looking back toward the source. The Thevenin voltage of the signal source is greater than the signal source output voltage when terminated in 50 Ω because R_T must always be greater than 50 Ω . In this case, R_T is 61.9 Ω and the Thevenin voltage and resistance are 2.2 V p-p and 28 Ω , respectively. Now the upper input branch can be viewed as a 2.2 V p-p source in series with 228 Ω . Because this is a unity-gain application, a 2 V p-p differential output is required, and R_F must therefore be $228 \times (2/2.2) = 206 \Omega$. The closest standard value to this is 205 Ω .

When generating the Typical Performance Characteristics data, the measurements were calibrated to take the effects of the terminations on the closed-loop gain into account.

Because this is a single-ended-to-differential application on a single supply, the input common-mode voltage swing must be checked. From Figure 64, $\beta = 0.52$, $V_{OCM} = 2.4\text{ V}$, and V_{ICM} is 1.1 V p-p swinging about ground. Using Equation 16, V_{ACM} is calculated to be 0.53 V p-p swinging about a baseline of 1.25 V, and the minimum negative excursion is approximately 1 V.

Exposed Paddle (EP)

The 8-lead SOIC and the 8-lead LFCSP have an exposed paddle on the bottom of the package. To achieve the specified thermal resistance, the exposed paddle must be soldered to one of the PCB planes. The exposed paddle mounting pad should contain several thermal vias within it to ensure a low thermal path to the plane.

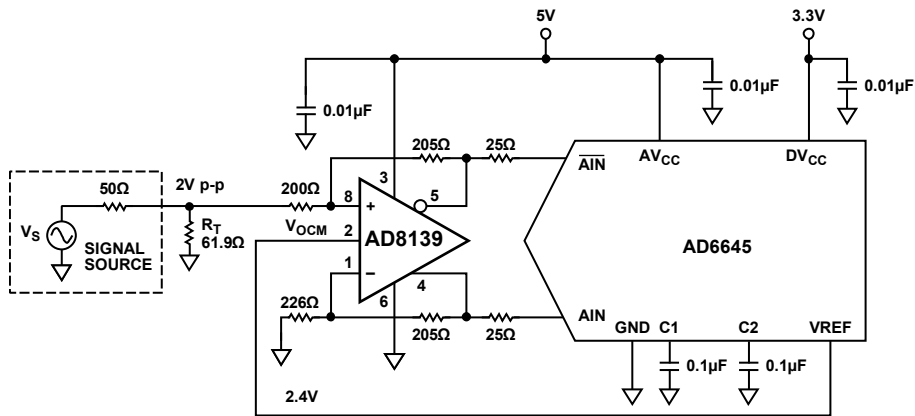
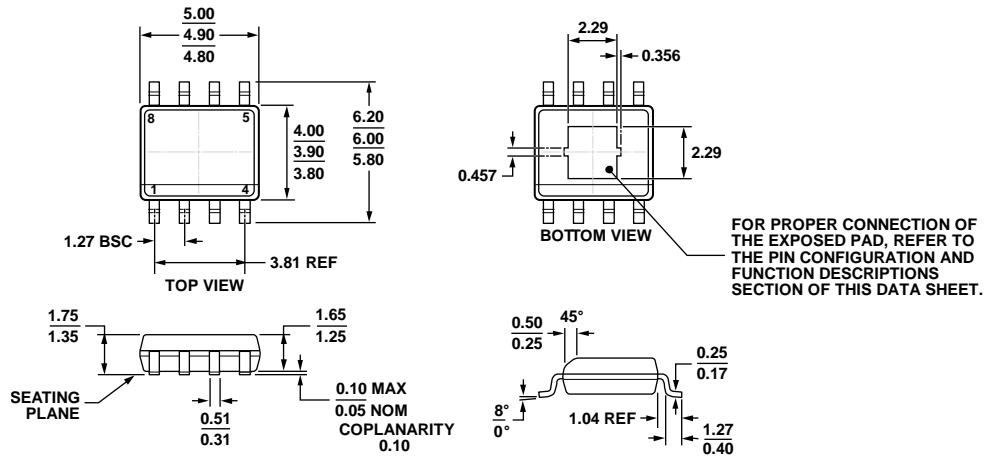


Figure 64. AD8139 Driving AD6645, 14-Bit, 80 MSPS/105 MSPS ADC

04679a-64

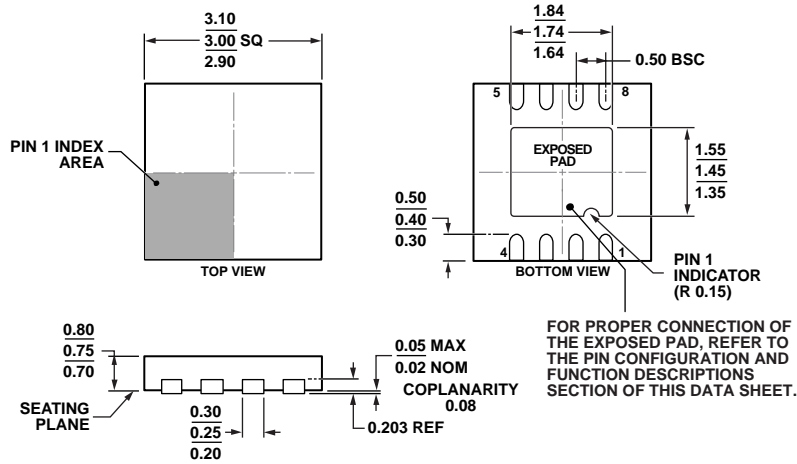
OUTLINE DIMENSIONS



COMPLIANT TO JEDEC STANDARDS MS-012-A A

Figure 65. 8-Lead Standard Small Outline Package with Exposed Pad [SOIC_N_EP] Narrow Body (RD-8-1)
Dimensions shown in millimeters

06-02-2011-B



COMPLIANT TO JEDEC STANDARDS MO-229-WEED

Figure 66. 8-Lead Lead Frame Chip Scale Package [LFCSP] 3 mm x 3 mm Body and 0.75 mm Package Height (CP-8-13)
Dimensions shown in millimeters

12-07-2010-A

ORDERING GUIDE

Model ¹	Temperature Range	Package Description	Package Option	Branding
AD8139ARDZ	-40°C to +125°C	8-Lead Small Outline Package with Exposed Pad [SOIC_N_EP]	RD-8-1	
AD8139ARDZ-REEL	-40°C to +125°C	8-Lead Small Outline Package with Exposed Pad [SOIC_N_EP]	RD-8-1	
AD8139ARDZ-REEL7	-40°C to +125°C	8-Lead Small Outline Package with Exposed Pad [SOIC_N_EP]	RD-8-1	
AD8139ACPZ-R2	-40°C to +125°C	8-Lead Lead Frame Chip Scale Package [LFCSP]	CP-8-13	HEB#
AD8139ACPZ-REEL	-40°C to +125°C	8-Lead Lead Frame Chip Scale Package [LFCSP]	CP-8-13	HEB#
AD8139ACPZ-REEL7	-40°C to +125°C	8-Lead Lead Frame Chip Scale Package [LFCSP]	CP-8-13	HEB#
AD8139ACP-EBZ		Evaluation Board		

¹ Z = RoHS Compliant Part, # denotes RoHS product may be top or bottom marked.

X-ON Electronics

Largest Supplier of Electrical and Electronic Components

Click to view similar products for [Differential Amplifiers](#) category:

Click to view products by [Analog Devices](#) manufacturer:

Other Similar products are found below :

[AD8206WHRZ](#) [LT6604IUFF-2.5#PBF](#) [LTC6419IV#PBF](#) [AD8479TRZ-EP](#) [INA149AMDREP](#) [INA146UA/2K5](#) [MAX9626ATC+](#)
[MAX4199ESA+](#) [INA132U/2K5](#) [INA105KU/2K5](#) [EL5375IUZ](#) [ADM1272-1ACPZ](#) [DC1538A](#) [LTC1992-10CMS8#PBF](#) [LTC1992CMS8#PBF](#)
[LT6375HMS#PBF](#) [LTC1992-2HMS8#PBF](#) [LTC1992-5HMS8#PBF](#) [LT6604IUFF-15#PBF](#) [AD8270ACPZ-R7](#) [LT6350IDD#PBF](#)
[AD8475ACPZ-R7](#) [LTC1992-1IMS8#PBF](#) [AD8476BRMZ-R7](#) [MAX9626ATC+T](#) [AD8132ARZ-RL](#) [LTC1992IMS8#PBF](#) [INA2132U/2K5](#)
[LT6600CS8-2.5#PBF](#) [LTC1992-10IMS8#PBF](#) [LTC1992-1HMS8#PBF](#) [LTC6605CDJC-7#PBF](#) [TDA8579T/N1SJ](#) [LTC1992-2CMS8#PBF](#)
[LT6604CUFF-5#PBF](#) [LTC6403CUD-1#PBF](#) [LT6350IMS8#PBF](#) [THS4552IRTWT](#) [LTC1992-2IMS8#PBF](#) [LTC1992HMS8#PBF](#)
[LT6350CMS8#PBF](#) [THS4551IRGTT](#) [AD8138SRMZ-EP-R7](#) [AD8138ARMZ-REEL](#) [AD8138ARZ-RL](#) [LT6350HMS8#PBF](#) [LTC6363IMS8-](#)
[0.5#PBF](#) [THS4551IRGTR](#) [LT1990IS8#PBF](#) [LT1995IDD#PBF](#)